

See discussions, stats, and author profiles for this publication at: <https://www.researchgate.net/publication/231277158>

Supercritical Water Oxidation of 2-Chlorophenol Catalyzed by Cu^{2+} Cations and Copper Oxide Clusters

ARTICLE *in* ENVIRONMENTAL SCIENCE AND TECHNOLOGY · OCTOBER 2000

Impact Factor: 5.33 · DOI: 10.1021/es001062s

CITATIONS

44

READS

27

2 AUTHORS:



Kuen-Song Lin

Yuan Ze University

94 PUBLICATIONS 1,056 CITATIONS

SEE PROFILE



Hong Paul Wang

National Cheng Kung University

184 PUBLICATIONS 2,722 CITATIONS

SEE PROFILE

Supercritical Water Oxidation of 2-Chlorophenol Catalyzed by Cu^{2+} Cations and Copper Oxide Clusters

KUEN-SONG LIN AND H. PAUL WANG*

Department of Environmental Engineering, National Cheng Kung University, Tainan City, Taiwan 70101, R.O.C.

Experimentally, the selectivity to decomposition (S/D) ($\text{S/D} = (\text{amount of 2-chlorophenol (2CP) oxidized to } \text{CO}_2 \text{ and } \text{H}_2\text{O}) / (\text{disappearance of 2CP})$) ratio for oxidation of 2CP with Cu^{2+} cations in supercritical water was greater than that without any catalysts by 60%. The enhancement was due to a fast precipitation of copper chloride in the supercritical water oxidation (SCWO) process. Formation of toxic byproducts was significantly reduced. Because of a confined environment in the channels of ZSM-5, formation of undesired heavy chlorinated phenols and PAH (polycyclic aromatic hydrocarbon) byproducts in the SCWO of 2CP (catalyzed by CuO/ZSM-5) was also highly suppressed. Only trace light-PAHs with a molecule size less than 6 Å were found in the SCWO of 2CP. Carcinogenic PAHs (heavy-PAHs) were not observed. The extended X-ray absorption fine structural (EXAFS) spectra of the catalyst showed that the copper oxides in the channels of ZSM-5 may form Cu_3O_2 clusters with Cu–Cu and Cu–O bond distances of 2.79 and 1.91 Å, respectively. The Cu_3O_2 clusters were oxidized to Cu_3O_4 by H_2O_2 in the supercritical water. Since the diffusion coefficients of copper oxide clusters (Cu_3O_4) in the channels of ZSM-5 was greater than that of 2CP by at least 3 orders, it is possible that these clusters are relatively mobile in ZSM-5 in the SCWO process.

Introduction

At supercritical conditions ($T > 647.3 \text{ K}$, $P > 22.1 \text{ MPa}$), water has a high solubility for both organics and oxygen (1, 2). Properties of supercritical water such as the complete miscibility in all proportions with oxygen, negligible surface tension, high diffusivity, low viscosity, and low solubility of inorganic salts are very unique especially in disposal of toxic compounds (1–5). Most hazardous organic compounds can be completely oxidized to CO_2 and H_2O in a very short residence time in the supercritical water (6–11). The desired destruction and removal efficiency (DRE) ($> 99.99\%$) may be achieved in seconds or minutes in the SCWO process (12–17).

2-Chlorophenol, widely used in paper, pulp, pesticide, and herbicide industries, is one of the EPA (Environmental Protection Agency) priority pollutants (18, 19). 2-Chlorophenol is very toxic and poorly biodegradable. Oxidation of 2CP in supercritical water is of practical interest since a wastewater stream containing 2CP over 200 ppm may not be treated effectively by direct biological methods (19).

Polycyclic aromatic hydrocarbons with two or more fused benzene rings are frequently found in the processes of

pyrolysis or incomplete combustion and carbonization of organic materials (20). Chlorine atoms may accelerate the abstraction of aromatic H from stable PAHs molecules that are activated for further mass growth of PAHs to form eventually soot (21). Many PAHs are toxic and considered as possible or probable carcinogens and/or mutagens (20). From an environmental viewpoint, complete destruction and removal of hazardous compounds with a minimal release of toxic byproducts are essential in the most waste disposal processes (20, 21).

Catalytic SCWO reactions are of interest to reduce the high temperature and pressure requirements of conventional SCWO processes. Because of the unique pore systems, zeolites have excellent shape selectivities in catalytic reactions (22–25). Since the zeolite ZSM-5 has a three-dimensional channel structure with pore sizes of 5.1–5.8 Å, the formation of high molecular weight hydrocarbons may be very limited (22–24). 2-Chlorophenol with the Lennard-Jones minimum kinetic diameter of 6.84 Å in size is tight-fit in the channels of ZSM-5. In a separate experiment, by FTIR spectroscopy, we have found that the channels of ZSM-5 were distorted by adsorbed benzene molecules that possessed a high symmetry of D_{6h} (26).

Reduction of undesired byproducts in the waste thermal treatment process effected by the shape selectivity of zeolite catalysts has not been extensively studied (22–25). Therefore, the main objective of the present work was to investigate the oxidation of 2CP in supercritical water and reduction of byproducts (higher chlorinated phenols and polycyclic aromatic hydrocarbons) in the SCWO of 2CP effected by Cu^{2+} cations as well as CuO/ZSM-5 . The nature of the active oxidative species (copper oxides) in the channels of ZSM-5 was also determined by X-ray absorption, X-ray photoelectron, electron paramagnetic resonance, and solid-state nuclear magnetic resonance spectroscopies.

Experimental Section

The SCWO experiments of 2CP (Merck, purity $> 99.5\%$) were conducted in a high-pressure quartz-lined batch and an isothermal, isobaric fixed-bed plug flow reactor (stainless steel 316 L type). The system pressure was controlled by a back-pressure regulator (Tescom, $P_{\text{max}} = 41.34 \text{ MPa}$) and a pressure regulator (Tescom, $P_{\text{in}} = 24.11 \text{ MPa}$; $P_{\text{out}} = 0.71 \text{ MPa}$). A safety rupture disk rated at 40.53 MPa was installed. Oxidation of 2CP in supercritical water was conducted at 673–773 K with the reaction residence times of 0.5–5 min. Concentrations of 2CP in the SCWO experiments were 189–1500 mg L^{-1} . Hydrogen peroxide (Merck, 30 wt %) was used as the oxidant ($\text{O/C ratio} = 0.95\text{--}2.0$) in the SCWO experiments. High purity copper acetate ($\text{Cu}(\text{CH}_3\text{COO})_2$) (Merck, purity $> 99\%$) was also used as the cation source (equivalent mole ratios ($[\text{Cu}]/[\text{Cl}]$) were 1.2–1.3) for the abstraction of Cl of 2CP in the SCWO process. The counteranion (CH_3COO^-) was decomposed in the SCWO process (7).

Zeolite ZSM-5 with the Si/Al ratio of 65 was prepared with fumed silica and organic template agent (tetrapropylammonium bromide, TPABr) hydrothermally. TPABr was a structure-directing agent. The zeolite syntheses were carried out at 383 K under the autogenous pressure of 15 atm for about 48 h. The CuO/ZSM-5 catalyst was prepared via ion exchange of zeolite ZSM-5 in a 0.01 N $\text{Cu}(\text{CH}_3\text{COO})_2$ aqueous solution for 24 h. The CuO/ZSM-5 was dried at 378 K for 16 h and calcined at 823 K for at least 6 h. About 3.1% Cu was loaded on ZSM-5. The CuO/ZSM-5 catalyst (0.15 g) was used in the SCWO of 2CP. Structures of samples were measured by X-ray powder diffraction (XRD) scanned from 5 to 80°

* Corresponding author phone: 011-8866-276-3608; fax: 011-8866-275-2790; e-mail: wanghp@mail.ncku.edu.tw.

(2 θ) with a scan rate of 4° (2 θ) min⁻¹ with monochromatic CuK α radiation (RIGAKU Model D/MAX III-V). The morphology of the salt precipitate was determined by scanning electron microscopy/energy dispersive spectroscopy (SEM/EDX, JEOL Model JSMr840). The average content of ZSM-5 was evaluated by atomic adsorption spectroscopy (AAS, HITACHI Model Z-8100) and induced couple plasma/mass spectroscopy (ICP/MS, ELAN model 5000). The Si/Al ratio of ZSM-5 was determined by X-ray fluorescence (XRF, RIGAKU Model 3063M). The pore volume (0.19 mL g⁻¹) and surface area (550 m² g⁻¹) of ZSM-5 were measured by nitrogen adsorption (Micromeritics ASAP 2010 Instrument) and mercury penetration (Micromeritics Autopore II 9220), respectively.

Carbon dioxide produced from the SCWO of 2CP passed through a water cooler and was measured by a totalizer and analyzed by *online* FTIR spectroscopy and gas chromatography (Perkin-Elmer Auto System) with a thermal conductive detector (GC/TCD) and a Supelco 60/80 Carboxen 1000 S.S. column. Overall carbon balance for the SCWO of 2CP was > 96%. Infrared spectra were recorded on a Digilab FTIR spectrometer (FTS-40) with fully computerized data storage and data handling capability. For all spectra reported, a 64-scan data accumulation was conducted at a resolution of 4 cm⁻¹.

Trace byproducts (extracted with a dichloromethane (Merck, purity > 99%) solvent) formed in the SCWO of 2CP was determined quantitatively by GC (Hewlett-Packard 5890A) with a mass selective detector (GC/MS, HP 5972) and an automatic sampler (HP-7673A). A HP Ultra 2 capillary column (50 m \times 0.32 mm \times 0.17 μ m) was heated programmably (323 K to 373 K at 20 K min⁻¹; 373 K to 563 K at 3.5 K min⁻¹; and hold at 563 K for 40 min) to 563 K to obtain a resolvable separation of PAH species. The injection temperature was 583 K. One to two microliters of sample was injected into column. Masses of primary and secondary ions of PAHs were determined using the scan-mode for PAH standards (Mix 610-M (Supelco, purity > 99%) and PNA-550JM (Chem Service, purity > 99%)) and samples. Analyses of trace byproducts of the SCWO of 2CP were also conducted by HPLC (spectra system, SP) with a 3-D UV detector (model UV-3000). PAHs were separated by a Spherisorb S5 PAH 5 μ m column (150 mm \times 4.6 mm) with a mixed acetonitrile/water mobile phase. Chlorinated phenols were analyzed by an Envirosep-PP column (125 mm \times 3.2 mm) with a mixed methanol/water (both with 1% acetic acid) mobile phase. A variable wavelength program was used in the system software (model PC-1000) to optimize detector sensitivity and selectivity.

²⁹Si solid-state nuclear magnetic resonance (SSNMR) spectra of the catalysts were recorded at 9.4 T and 79.0 MHz on a Bruker Avance DSX 400 solid-state NMR spectrometer. Tetramethylsilane was used as chemical shift references (external standard) for ²⁹Si. Bruker double-bearing channel 4 or 7 mm (O.D.) MAS probes and zirconia rotors were used and spun at a frequency of 5 kHz at the magic angle. Dry air was used as the driving and bearing gas in the SSNMR experiments. In all cases a background signal was subtracted from the spectra. The recycle delay was 10 s with a pulse width of 3.0 μ s (about 60° (flip angle)) for ²⁹Si.

X-ray photoelectron spectra (XPS) of the CuO/ZSM-5 catalysts were measured on a Fison ESCA 210 (VG Scientific) spectrometer with a MgK α X-ray (1253.6 eV) excitation source. The binding energy (E_b) of the Cu 2P_{3/2} line was calibrated with that of O 1s (530.8 and 532.5 eV) and C 1s (284.4 eV) lines. The E_b (copper core level binding energy) value of electrons emitted by L₃M_{4,5}M_{4,5} transition was used for copper species. The standard deviation of the binding energy (E_b) measurement was \pm 0.3 eV typically.

TABLE 1. Trace PAH and Chlorinated Phenols Byproducts Formed in the SCWO of 2CP with 0.02 N Cu²⁺ and CuO/ZSM-5 at 673 K for 1 Min in a Fixed-Bed Plug Flow Reactor (O/C Ratio = 1.1)

	minimum size ^a (Å)	(μ g (g 2CP) ⁻¹)			
		no catal.	Cu ²⁺	CuO/ZSM-5	Cu ²⁺ +CuO/ZSM-5
S/D ^b		0.43	0.97	0.86	0.99 ⁺
2CP conversion		0.98	0.99	0.99	0.99 ⁺
phenol	5.85	1370	164.7	165.6	7.5
2,4-DCP	6.84	2590	21.9	20.5	1.7
2,4,5-TCP	7.75	5735	10.3	0.2	N.D. ^c
2,4,6-TCP	7.75	7056	11.2	N.D. ^c	N.D. ^c
2,3,4,6-TeCP	7.75	2101	1.4	N.D. ^c	N.D. ^c
PCP	7.75	159	N.D. ^c	N.D. ^c	N.D. ^c
naphthalene	5.85	25.6	4.4	6.4	1.0
fluorene	5.85	3.3	0.3	1.0	0.1
phenanthrene	9.10	4.0	N.D. ^c	0.1	N.D. ^c
anthracene	5.85	3.2	0.1	1.6	0.1
fluoranthene	9.45	1.2	N.D. ^c	N.D. ^c	N.D. ^c
pyrene	9.10	0.8	N.D. ^c	N.D. ^c	N.D. ^c
benz[a]anthracene	9.10	1.8	N.D. ^c	0.1	N.D. ^c
chrysene	9.10	0.3	N.D. ^c	N.D. ^c	N.D. ^c
benzo[b]fluoranthene	9.10	0.2	0.1	0.1	N.D. ^c
benzo[k]fluoranthene	9.10	N.D. ^c	N.D. ^c	N.D. ^c	N.D. ^c
benzo[a]pyrene	9.10	0.5	N.D. ^c	N.D. ^c	N.D. ^c
indeno[1,2,3-cd]pyrene	9.45	0.16	N.D. ^c	N.D. ^c	N.D. ^c
dibenz[a,h]anthracene	9.45	N.D. ^c	N.D. ^c	N.D. ^c	N.D. ^c
benzo[ghi]perylene	9.45	N.D. ^c	N.D. ^c	N.D. ^c	N.D. ^c

^a The Lennard-Jones minimum kinetic diameter (22–24). ^b S/D = (amount of 2CP oxidized to CO₂ and H₂O)/(disappearance of 2CP). ^c N.D. denotes "not detectable".

The electron paramagnetic resonance (EPR) spectra of the catalysts were recorded on a Bruker Model EMX-10 EPR spectrometer with a maximum microwave power of 200 mW at 77–463 K. About 30–60 mg of the catalyst samples in the quartz tube (5 mm O.D.) were measured. The magnetic field was modulated at 100 kHz. Diphenylpicrylhydrazyl (DPPH) was used for determination of the absolute *g*-factor (*g* = 2.0037). All EPR spectra were normalized to the same frequency, sample weight, and spectrometer gain.

The extended X-ray absorption fine structural (EXAFS) spectra were collected on a bending-magnet double-crystal monochromator (DCM) X-ray beamline in the Synchrotron Radiation Research Center (SRRC) of Taiwan. The electron storage ring was operated with an energy of 1.5 GeV and a current of 100–200 mA. A Si(111) DCM was used for providing highly monochromatized photon beams with energies of 1 to 9 keV and resolving power (*E*/ Δ *E*) of up to 7000. Data were collected in fluorescence mode with a Lytle detector (27) for the Cu K-edge (8978.9 eV) experiments. The absorption spectra were collected in ion chambers filled with helium gas. The photon energy was calibrated by characteristic preedge peaks in the absorption spectrum of a copper foil. The raw absorption data in the region of 50 to 200 eV below the edge position were fit to a straight line using the least-squares algorithms. The fitted preedge background curves were extrapolated throughout all data range and subtracted and normalized to minimize the effect of sample thickness. The near-edge spectra were ranged between the threshold and the point at which the EXAFS began (27–32). The X-ray absorption near edge structural (XANES) spectra extend to an energy of 50 eV above the edge. The *k*²-weighted EXAFS spectra were Fourier transformed to *R* space over the range between 2.5 and 10.8 Å⁻¹. The EXAFS data were analyzed using the UWXAFS 3.0 and FEFF 8.0 programs (29–32).

Results and Discussion

Cu(II) Cations Catalysis. Table 1 shows that oxidation of 2CP in supercritical water was enhanced (S/D = 0.97) by

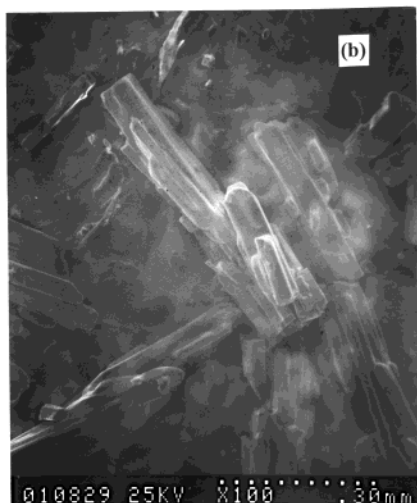
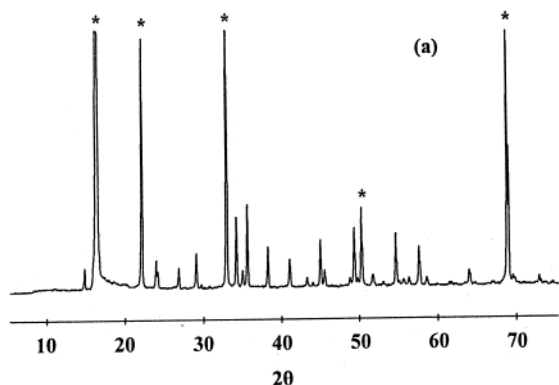


FIGURE 1. (a) X-ray diffraction pattern and (b) scanning electron microscopy/energy dispersive spectrum of CuCl_2 salt precipitated in the SCWO of 2CP in the presence of Cu^{2+} (fixed-bed plug flow reactor). An asterisk (*) denotes the characteristic peaks of CuCl_2 .

Cu^{2+} cations (if compared with that without any cations). The enhancement was about 60%. Reduction of highly chlorinated phenol and PAH byproducts formed in the SCWO of 2CP with Cu^{2+} cations is also shown in Table 1. The reduction of these toxic byproducts may be due to the fact that the electron-withdrawing effect of cations was involved in which an intermediate species ($(\text{OH})\text{PhCl}^{3-} - \text{Cu}^{3+}$) might exist. In addition, due to the extremely low solubility of salts in the supercritical water, abstraction of Cl from 2CP and formation of the copper chloride precipitate may be involved in the early stage of the SCWO process. Figure 1 shows that by using XRD and SEM/EDX spectroscopies, CuCl_2 was the main species in the precipitate in the SCWO of 2CP at 673 K for 1 min. Over 85% of Cu^{2+} cations was formed as CuCl_2 in the SCWO of 2CP. Solubility of copper chloride has been reported to decrease from its ambient solubility (298 K, 0.10 MPa) of about 10% to 3–120 ppm in supercritical water (773 K, 25.33 MPa), a decrease of 10^4 -fold (3–5).

Byproducts Shape Selective Catalysis. The unique byproduct selectivity for oxidation of 2CP in supercritical water effected by the $\text{CuO}/\text{ZSM-5}$ catalyst is also shown in Table 1. In the tight-fit channels of ZSM-5, the S/D ratio for the SCWO of 2CP at 673 K was 0.86, that may be due to the fact that an extremely high collision frequency of 2CP with the active copper species may occur in the channels of ZSM-5. In the presence of both Cu^{2+} cations and the zeolite catalyst, the S/D ratio for the SCWO of 2CP was notably enhanced (>0.99). Without the zeolite catalyst, 2,4-dichlorophenol (2,4-DCP) and 2,4,5-trichlorophenol (2,4,5-TCP) were the main chlorinated phenols formed in the SCWO of 2CP at 673 K. Due to the restricted environment in the channels of ZSM-5,

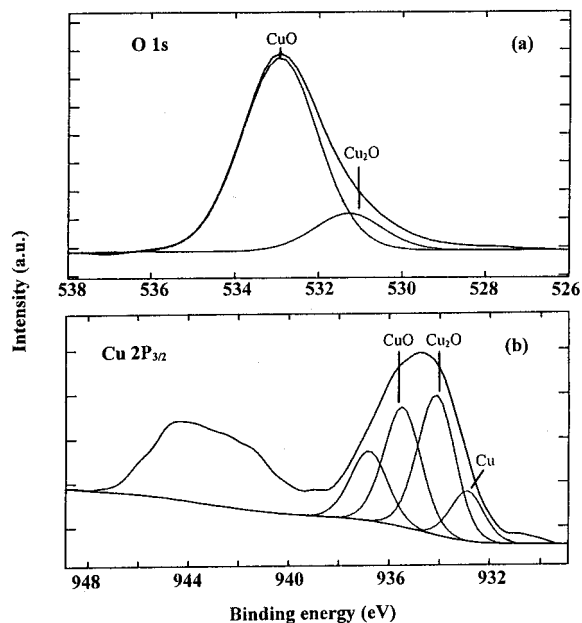


FIGURE 2. XPS spectra of (a) O 1s and (b) Cu $2\text{P}_{3/2}$ of the used $\text{CuO}/\text{ZSM-5}$ catalyst for the SCWO of 2CP at 673 K for 1 min (O/C ratio = 1.1; concentration of 2CP = 1500 mg L^{-1}).

SCHEME 1

By-product	Conc. ($\mu\text{g/g}$ 2CP)
2,4-DCP	20.5
2,4,5-TCP	0.2
2,4,6-TCP	N.D.
2,3,4,6-TcCP	N.D.
PCP	N.D.

ZSM-5 channels (5.1–5.8 Å)

* Denotes the possible Cl reinsertion sites.

the Cl-reinsertion may occur most likely at the sites #4 and #5 of 2CP (Scheme 1). Therefore, large molecules such as 2,3,4,6-tetrachlorophenol (2,3,4,6-TCP) and pentachlorophenol (PCP) were not formed. Note that reactions of ring-opening, in which products are ultimately oxidized to CO_2 and H_2O , are predominant in the overall reaction. The high-chlorinated phenol byproducts formed in the SCWO of 2CP were, in fact, extremely low (0.2 to $20.5 \mu\text{g (g 2CP)}^{-1}$).

Furthermore, due to the byproduct shape selectivity in the channels of ZSM-5, the formation of high-molecular-weight PAHs was also very limited (Table 1). Formation of PAHs in the SCWO of 2CP in ZSM-5 was significantly suppressed. Mainly low-molecular-weight PAHs (or light PAHs) such as naphthalene (Nap), fluorene (Flu), and anthracene (Ant) were formed in the SCWO of 2CP. Carcinogenic heavy PAHs including benzo[a]pyrene (BaP), benzo[b]fluoranthene (BbF), chrysene (CHR), dibenz[a,h]anthracene (DBA), and benzo[ghi]perylene (BghiP) were not found in the SCWO of 2CP.

Nature of Copper Oxides in ZSM-5. To more thoroughly examine the nature of the copper species in ZSM-5, XPS spectra of the catalyst were measured and calculated (33, 34). The O 1s spectrum of the $\text{CuO}/\text{ZSM-5}$ catalyst (Figure 2(a)) indicates the existence of at least two oxidation states (Cu_2O and CuO) in ZSM-5. The CuO-to- Cu_2O ratio was 2.1 ± 0.3 . In addition, in Figure 2(b), three oxidation states such as Cu, Cu(I) (Cu_2O), and Cu(II) (CuO) are also observed in the Cu $2\text{P}_{3/2}$ spectra. About 13% of metallic Cu was found in the $\text{CuO}/\text{ZSM-5}$ catalyst (Table 2). The Cu(II) species

TABLE 2. Fractions of Copper Species (Cu 2P_{3/2}) in the Used CuO/ZSM-5 Catalyst^a

	Cu	Cu ₂ O	CuO
bonding energy (eV)	933.4	932.0	935.6
fraction (%)	13.1	25.7	61.2

^a SCWO of 2CP at 673 K for 1 min with O/C ratio of 1.1.

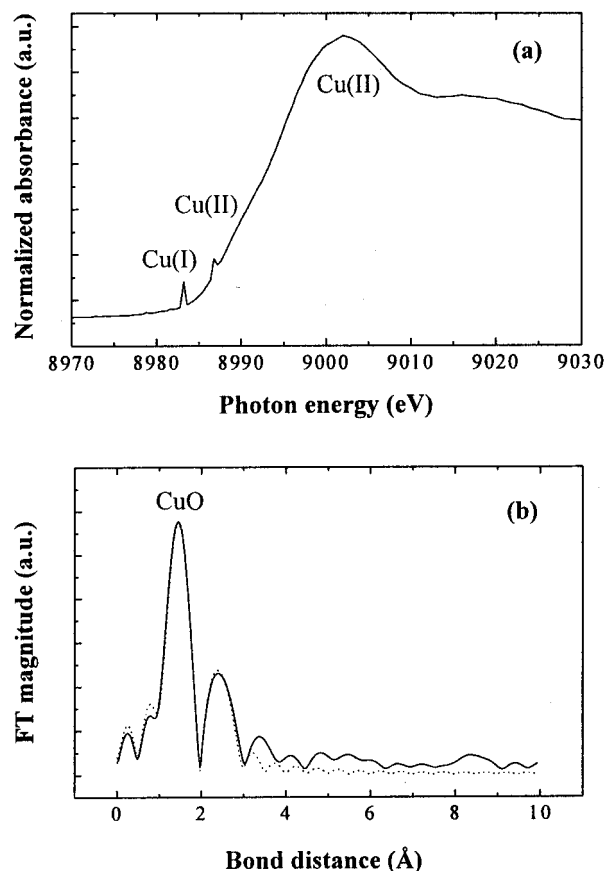


FIGURE 3. (a) XANES and (b) Fourier transform (FT) of the Cu K-edge EXAFS oscillation $k^2\chi(k)$ of the used CuO/ZSM-5 catalyst for the SCWO of 2CP at 673 K for 1 min (O/C ratio = 1.1; concentration of 2CP = 1500 mg L⁻¹). The best fittings of the EXAFS spectra are expressed by the dotted lines.

originally in the CuO/ZSM-5 catalyst might be reduced to Cu(I) and metallic Cu in the SCWO process. The Cu(I) and metallic Cu species might be reoxidized by the oxidant (H₂O₂) in supercritical water.

To further investigate the structure of the active copper species in ZSM-5, X-ray absorption spectra of the catalyst were also measured (26–32). The XANES spectrum of the CuO/ZSM-5 catalyst used in the SCWO of 2CP is shown in Figure 3(a). The preedge XANES spectrum of CuO/ZSM-5 exhibits very weak absorbance feature for the 1s to 3d transition which is forbidden by the selection rule in the case of perfect octahedral symmetry. The sharp feature at 8982–8984 eV, due to the dipole-allowed of 1s to 4p_{xy} electron transition, indicates the existence of Cu(I). The intensity of the 1s to 4p_{xy} transition is proportional to the population of Cu(I) in ZSM-5. A shoulder at 8985–8988 eV and an intense feature at 8994–8997 eV are attributed to the 1s to 4p_{xy} transition that indicates the existence of Cu(II) species in the channels of ZSM-5. The XANES spectra work particularly well in distinguishing of Cu(I) and Cu(II) coexisted in the channels of ZSM-5.

TABLE 3. Fine Structural Parameters of CuO/ZSM-5 Used in the SCWO of 2CP at 673 K for 1 Min with O/C Ratio of 1.1

	shell	CN ^a	R ^b (±0.05 Å)	Δσ ^{2 c} (Å ²)
Cu₃O₂ Cluster				
Cu–O	first	2.5	1.91	0.008
	second	2.1	3.61	0.015
Cu–Cu	first	4.0	2.79	0.016
	second	5.6	4.41	0.021
Cu₃O₄ Cluster				
Cu–O	first	2.6	1.89	0.008
	second	2.1	3.54	0.015
Cu–Cu	first	4.4	2.80	0.013
	second	5.5	4.53	0.019

^a CN: coordination number. ^b R: bond distance. ^c σ: Debye–Waller factor.

Generally, the EXAFS spectroscopy can provide the information on the atomic arrangement of catalysts in terms of bond distance, number and kind of near neighbors, thermal and static disorder. An over 99% reliability of the EXAFS data fitting for Cu species in zeolite was obtained (Figure 3(b)). The Fourier transformation was performed on k^2 -weighted EXAFS oscillations over the range between 2.5 and 10.8 Å⁻¹. Standard deviation calculated from the averaged spectra was also determined. In all EXAFS data analyzed, the Debye–Waller factors (Δσ²) were less than 0.02 Å² (Table 3).

Since interactions between Cu and Si or Al (second shell) were not observed by EXAFS, it is possible that copper oxide clusters may be formed in the channels of ZSM-5. The structural parameters of the copper oxide clusters obtained from the best fit to the EXAFS data are shown in Table 3. The postulated structure of the copper oxide clusters involved in the SCWO of 2CP in the channels of ZSM-5 was Cu₃O₂. The Cu–O and Cu–Cu species with bond distances of 1.91 and 2.79 Å, respectively, were found. Coordination number (CN) of the Cu–O species was 2.5. The Cu₃O₂ clusters were oxidized by H₂O₂ to form Cu₃O₄ clusters with Cu–Cu and Cu–O bond distances of 2.80 and 1.89 Å, respectively. Coordination number of the Cu–O species was 2.6. Note that chlorine-bonded CuO species in the channels of ZSM-5 was not observed by EXAFS spectroscopy. Thus, one may eliminate the possibility that copper species of the clusters was involved in the abstraction of Cl from 2CP in the SCWO process.

In addition, ²⁹Si solid-state NMR spectra of the CuO/ZSM-5 catalysts used in the SCWO of 2CP are shown in Figure 4. The feature at (–114) – (–103) ppm represents the Q₄ sites where all of the second-nearest neighbor atoms are Si. Instead of interaction with ZSM-5, copper oxide species was mechanically supported on zeolites. Interactions of the copper species with the =Si–O–Al= sites on ZSM-5 seem to be insignificant.

Electron paramagnetic resonance spectroscopy has been used to investigate the structural environment of paramagnetic copper species in zeolites (35–41). Determining the motion, location, and coordination of copper species in the channels of zeolite catalysts is acute to understanding the role of copper species in the SCWO of 2CP. The EPR spectra of the CuO/ZSM-5 catalyst measured at 77, 298, and 463 K (Figure 5) indicate that the copper oxide species has a square-plane structure in the channels of ZSM-5. The EPR spectrum (Figure 5(c)) of the CuO/ZSM-5 catalyst at 463 K is broad and structureless. On the contrary, at 77 K, the spectrum (Figure 5(a)) exhibits a sharp signal and characteristic structure of copper oxide complexes that the hyperfine coupling between the 3d unpaired electrons and the copper (I = 3/2) nuclear spin is well resolved. Furthermore, the broad EPR spectrum observed at 463 K in Figure 5(c) suggests that the copper oxide species may be mobile in the channels of ZSM-5. At 77 K, the appearance of the parallel edges in the EPR spectrum

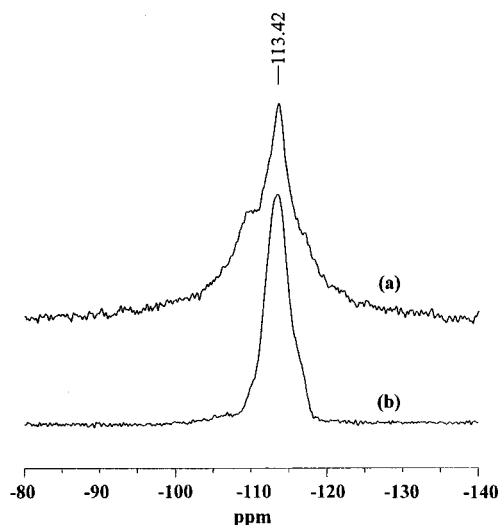


FIGURE 4. ^{29}Si SSNMR spectra of (a) fresh and (b) used CuO/ZSM-5 in the SCWO of 2CP (O/C ratio = 1.1; concentration of 2CP = 1500 mg L^{-1}).

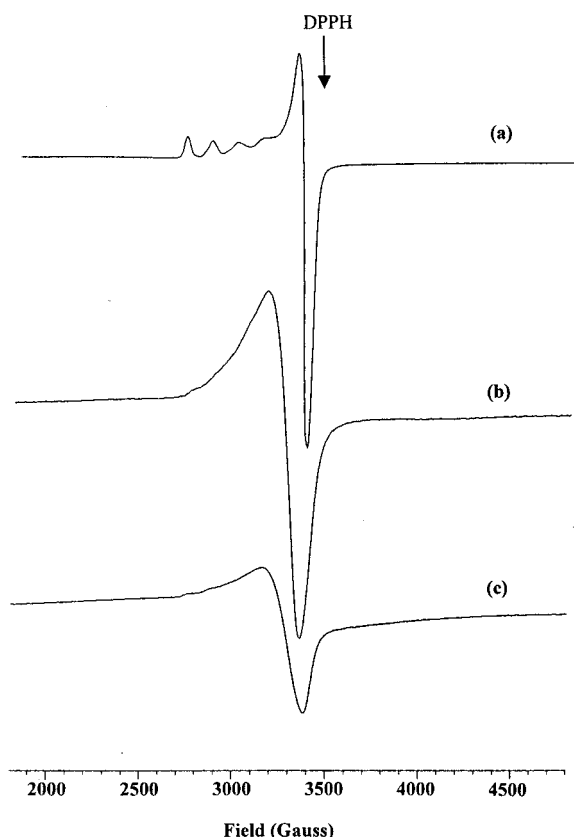


FIGURE 5. EPR spectra of the used CuO/ZSM-5 catalysts for the SCWO of 2CP at 673 K for 1 min (O/C ratio = 1.1; concentration of 2CP = 1500 mg L^{-1}) measured at (a) 77, (b) 298, and (c) 463 K ($\nu_{\text{EPR}} = 9.784 \text{ GHz}$, Field (Gauss) = 3475 or $g_{\text{DPPH}} = 2.0037$).

is observed in Figure 5(a) that indicates a reduced mobility of copper species in ZSM-5 at low temperatures. The features in the low-field region of the EPR spectra progressively shift when the catalyst was heated from 77 to 463 K. The observed changes in the EPR signal were reversible.

The diffusion coefficients of copper oxide clusters in the channels of ZSM-5 was calculated with the intensities of Cu EPR signals at 77–463 K. Furthermore, the diffusion coefficients of 2CP molecules in ZSM-5 were also derived from their molecular weight and diameters. In addition, by using

the equation $D = kD_c(T/M)^{1/2}$ (D_c is the channel factor depending on the zeolite pore sizes; T is temperature in K; M is the molecular weight; and k is a parameter) (22–24), the diffusion coefficient of the copper oxide cluster (Cu_3O_4 , at 673 K) was $1.10 \times 10^{-8} \text{ m}^2 \text{ s}^{-1}$ and was greater than that of 2CP by at least 3 orders. Note it is evident that the EPR signals were associated with perhaps all of the copper species introduced into zeolite by ion exchange and were representative of all the Cu(II) in ZSM-5.

In summary, due to an effective abstraction of Cl from 2CP by Cu^{2+} cations and an enhanced precipitation of copper chloride in the SCWO process, formation of toxic byproducts was significantly reduced. In the highly restricted environment of ZSM-5 channels, formation of higher chlorinated phenols and heavy PAH byproducts was also extremely limited in the SCWO of 2CP at 673 K. Only trace light-PAHs with a molecule size less than 6 Å were formed in the SCWO of 2CP. The copper oxides in the channels of ZSM-5 may form Cu_3O_2 clusters that were oxidized to form Cu_3O_4 clusters by H_2O_2 . In the channels of ZSM-5, diffusion coefficients of the copper oxide clusters were greater than that of 2CP by at least 3 orders. Since the reaction rate in supercritical water was extremely rapid, one may postulate that relatively mobile clusters (in the channels of ZSM-5) are involved in the SCWO of 2CP.

Acknowledgments

The financial support (1997–1999) of the National Science Council of Taiwan is gratefully acknowledged. We also thank Prof. Y. W. Yang and Dr. J. F. Lee of the Taiwan Synchrotron Radiation Research Center for their help in the EXAFS experiments and Ms. Ru-Rong Wu of the National Cheng Kung University for her SSNMR experimental assistance.

Literature Cited

- (1) Modell, M. In *Standard Handbook of Hazardous Waste Treatment and Disposal*; Freeman, H. M., Ed.; McGraw-Hill: New York, 1989; Sec. 8.11, p 153.
- (2) Shaw, R. W.; Brill, T. B.; Clifford, A. A.; Eckert, C. A.; Franck, E. U. *Chem. Eng. News* **1991**, 69, 26.
- (3) Fernández, D. P.; Goodwin, A. R. H.; Lemmon, E. W.; Levelt Sengers, J. M. H.; Williams, R. C. *J. Phys. Chem. Ref. Data* **1997**, 26, 1125.
- (4) Li, L. X.; Gloyna, E. F. *Sep. Sci. Technol.* **1999**, 34, 1463.
- (5) Huang, Y.-J.; Wang, H.-P.; Li, C.-T.; Chien, Y.-C. *Chemosphere* **2000**, 40, 347.
- (6) Li, R.; Savage, P. E.; Szmukler, D. *AIChE J.* **1993**, 39, 178.
- (7) Savage, P. E.; Smith, M. A. *Environ. Sci. Technol.* **1995**, 29, 216.
- (8) Lin, K. S.; Wang, H. P.; Li, M. C. *Chemosphere* **1998**, 36, 2075.
- (9) Lin, K. S.; Wang, H. P.; Yang, Y. W. *Chem. Lett.* **1998**, 1203.
- (10) Lin, K. S.; Wang, H. P.; Yang, Y. W. *Chemosphere* **1999**, 39, 1385.
- (11) Lin, K. S.; Wang, H. P. *Appl. Catal. B: Environ.* **1999**, 22, 261.
- (12) Lin, K. S.; Wang, H. P. *Environ. Sci. Technol.* **1999**, 33, 3278.
- (13) Chien, Y.-C.; Wang, H. P.; Lin, K. S.; Huang, Y.-J.; Yang, Y.-W. *Chemosphere* **2000**, 40, 383.
- (14) Lin, K. S.; Wang, H. P. *Langmuir* **2000**, 16, 2627.
- (15) Chien, Y.-C.; Wang, H. P.; Lin, K. S. *Water Res.* **2000**, 34, 4279.
- (16) Ding, Z. Y.; Aki, S. N. V. K.; Abraham, M. A. *Environ. Sci. Technol.* **1995**, 29, 2748.
- (17) Zhang, X.; Savage, P. E. *Catal. Today* **1998**, 40, 333.
- (18) Alejandro, A.; Medina, F.; Fortuny, A.; Salagre, P.; Sueiras, J. E. *Appl. Catal. B: Environ.* **1998**, 16, 53.
- (19) Krajnc, M.; Levec, J. *Ind. Eng. Chem. Res.* **1997**, 36, 3439.
- (20) Yu, J.; Savage, P. E. *Ind. Eng. Chem. Res.* **1999**, 38, 3793.
- (21) Aki, S. N. V. K.; Abraham, M. A. *Ind. Eng. Chem. Res.* **1999**, 38, 358.
- (22) Martino, C. J.; Savage, P. E. *Ind. Eng. Chem. Res.* **1999**, 38, 1775.
- (23) Martino, C. J.; Savage, P. E. *Environ. Sci. Technol.* **1999**, 33, 1911.
- (24) Atwater, J. E.; Akse, J. R.; McKinnis, J. A.; Thompson, J. O. *Chemosphere* **1997**, 34, 203.
- (25) Kaune, A.; Lenoir, D.; Schramm, K. W.; Zimmermann, R.; Kettrup, A.; Jaeger, K.; Ruckel, H. G.; Frank, F. *Environ. Eng. Sci.* **1998**, 15, 85.

- (19) Callahan, M. A.; Slimak, M. W.; Gabel, N. W.; May, I. P.; Fowler, C. F.; Freed, J. R.; Jennings, P.; Durfee, R. L.; Whitmore, F. C.; Maestri, B.; Mabey, W. R.; Holt, B. R.; Gould, C. *Water-related Environmental Fate of 129 Priority Pollutants*; U.S. Environmental Protection Agency: Washington, DC, 1979; EPA-440/4-79-029b; Vol. II, p 84-1-8.
- (20) Yasuda, K.; Takahashi, M. *J. Air Waste Manage. Assoc.* **1998**, *48*, 441.
- (21) Bjørseth, A. *Handbook of Polycyclic Aromatic Hydrocarbons*, 2nd ed.; Marcel Dekker: New York, 1983; p 34.
- (22) Breck, D. W. *Zeolite Molecular Sieves*, 1st ed.; John Wiley & Sons: New York, 1974; p 634.
- (23) Szostak, R. *Molecular Sieves Principles of Synthesis and Identification*, 1st ed.; Van Nostrand Reinhold: New York, 1989; p 51.
- (24) Lee, C. K.; Chiang, A. S. T.; Wu, F. W. *AIChE J.* **1992**, *38*, 128.
- (25) Wang, H. P.; Lin, K. S.; Huang, Y. J.; Li, M. C.; Tsaur, L. K. *J. Hazard. Mater.* **1998**, *58*, 147.
- (26) Wang, H. P.; Yu, T.; Garland, B. A.; Eyring, E. M. *Appl. Spectrosc.* **1990**, *44*, 1070.
- (27) Meitzner, G.; Via, G. H.; Lytle, F. W.; Sinfelt, J. H. *J. Phys. Chem.* **1992**, *96*, 4960.
- (28) Kumashiro, R.; Kuroda, Y.; Nagao, M. *J. Phys. Chem. B* **1999**, *103*, 89.
- (29) Rehr, J. J.; Stern, E. A. *Phys. Rev. B* **1976**, *14*, 4413.
- (30) Zabinsky, S. I.; Rehr, J. J.; Ankudinov, A.; Albers, R. C.; Eller, M. *J. Phys. Review B—Condensed Matter* **1995**, *52*, 2995.
- (31) Hoffmann, M. M.; Darab, J. G.; Palmer, B. J.; Fulton, J. L. *J. Phys. Chem. A* **1999**, *103*, 8471.
- (32) Korshin, G. V.; Frenkel, A. I.; Stern, E. A. *Environ. Sci. Technol.* **1998**, *22*, 2699–2705.
- (33) Jirka, I.; Bosáček, V. *Zeolites* **1991**, *11*, 77.
- (34) Chusuei, C. C.; Brookshier, M. A.; Goodman, D. W. *Langmuir* **1999**, *15*, 2806.
- (35) Larsen, S. C.; Aylor, A.; Bell, A. T.; Reimer, J. A. *J. Phys. Chem.* **1994**, *98*, 11533.
- (36) Kucherov, A. V.; Gerlock, J. L.; Jen, H. W.; Shelef, M. *J. Phys. Chem.* **1994**, *98*, 4892.
- (37) Carl, P. J.; Larsen, S. C. *J. Catal.* **1999**, *182*, 208.
- (38) Weil, J. A.; Bolton, J. R.; Wertz, J. E. *Electron Paramagnetic Resonance-Elementary Theory and Practical Applications*; John Wiley & Sons: New York, 1994; p 294.
- (39) Anderson, M. W.; Kevan, L. *J. Phys. Chem.* **1987**, *91*, 4174.
- (40) Kucherov, A. V.; Slinkin, A. A. *J. Phys. Chem.* **1989**, *93*, 864.
- (41) Dyrek, K.; Adamski, A.; Sojka, Z. *Spectrochim. Acta Part A-Molecular Biomolecular Spectrosc.* **1998**, *54*, 2337.

Received for review March 1, 2000. Revised manuscript received August 24, 2000. Accepted August 30, 2000.

ES001062S